PROCEEDINGS A

rspa.royalsocietypublishing.org

Research

Cite this article: Grima JN, Bajada M, Scerri S, Attard D, Dudek KK, Gatt R. 2015 Maximizing negative thermal expansion via rigid unit modes: a geometry-based approach. *Proc. R. Soc. A* **471**: 20150188.
http://dx.doi.org/10.1098/rspa.2015.0188

Received: 16 March 2015
Accepted: 28 May 2015

Subject Areas:
materials science

Keywords:
negative thermal expansion, thermal contraction, auxetic, negative Poisson's ratio

Author for correspondence:
J. N. Grima
e-mail: auxetic@um.edu.mt

Maximizing negative thermal expansion via rigid unit modes: a geometry-based approach

J. N. Grima[1,2], M. Bajada[1], S. Scerri[1], D. Attard[2], K. K. Dudek[2] and R. Gatt[2]

[1]Department of Chemistry, and [2]Metamaterials Unit, Faculty of Science, University of Malta, Msida MSD 2080, Malta

Existent rigid unit mode (RUM) models based on rotating squares, which may explain the phenomenon of negative thermal expansion (NTE), are generalized so as to assess the NTE potential for novel systems made from rectangular or rhombic rigid units. Analytical models for the area coefficients of thermal expansion (CTE) of these innovative networks are derived in an attempt to determine the optimal geometrical parameters and connectivity for maximum NTE. It was found that all systems exhibit NTE, the extent of which is determined by the shape and connectivity of the elemental rigid units (side lengths ratio or internal angle). It was also found that some of the networks proposed here should exhibit significantly superior NTE properties when compared with the well-known network of squares, and that for optimal NTE characteristics, pencil-like rigid units should be used rather than square-shaped ones, as these permit larger pore sizes that are more conducive to NTE. All this compliments earlier work on the negative Poisson's ratio (auxetic) potential of such systems and may provide a route for the design of new materials exhibiting superior thermo-mechanical characteristics including specifically tailored CTEs or giant NTE characteristics.

1. Introduction

The changes in size that occur when materials are subjected to a variation in temperature are quantified through their *coefficients of thermal expansion* (CTEs), parameters which typically assume a positive value as most materials expand in size upon heating. Nevertheless, *negative thermal expansion* (NTE) (or *thermal*

THE ROYAL SOCIETY PUBLISHING

contraction) is also possible, and describes a phenomenon by which a structure or material shrinks, at least in one direction, when subjected to an increase in temperature [1]. Owing to their intriguing, counterintuitive properties and attractive features for use in numerous applications, popularity in the field of NTE has grown tremendously in the past decades. Solid materials reported to exhibit this effect include quartz and vitreous silica [2], metal oxides [3–14], polymers and other organic-based compounds [15–17], zeolites [18–23] and metal-organic frameworks (MOFs) [24–27]. A key area of research is linked to the production and design of composite materials having an overall CTE that is tailored to a specific value [28]. Of particular interest in this respect are zero composite materials, that is materials composed of negatively and positively expanding materials in the correct ratio, which effectively result in a net thermal expansion coefficient of zero [29,30]. These invar-like materials which are unaffected by temperature changes have important applications in various fields [31], such as optics [32,33] and electronics [34].

Theoretical [35–38], computational [39,40] and experimental [5,41–43] studies have all contributed towards the discovery and categorization of the various NTE materials into a number of groups or families according to the mechanisms by which they deform. One of the most studied mechanisms within this domain is that of the 'rigid unit mode (RUM)' approach [44–48]. In essence, this extremely elegant concept is based on modelling the NTE capabilities of fully open, two-dimensional framework structures, composed of rigid units, under the thermal excitation of low frequency phonon modes (or RUMs). Such modes lead to a 'rocking-type motion' of the units and, hence, a subsequent shrinkage in the unit cell. A particularly appealing aspect of this approach is its elegance, as the model is mainly reliant on the geometric description of the material. More importantly, despite their simplicity, such models have been found to successfully explain the experimentally measured NTE in a number of classes of materials, such as β-quartz [47], whereupon some two-dimensional projections of the three-dimensional framework of the material were found to be adequately representable through a network of connected squares, and tridymite [49], which was modelled through an equivalent approach using a 'rotating rigid triangles' model.

Despite all this, it is unfortunate that the current models have only been rigorously developed for certain highly symmetric geometries, namely the aforementioned 'rotating squares' and 'rotating equilateral triangles' arrays. While these highly symmetric models are extremely useful to prove that one can achieve NTE through a RUMs approach, they are limited from various aspects. For example, as a result of their very high symmetry, they might not be applicable to represent the whole spectrum of materials which could potentially exhibit NTE as a result of RUMs. Furthermore, the symmetry leads to a reduction with regard to the generality of the models. From a mathematical point of view, these models may not be easily adaptable to study the effect that a change in the geometry may have on the extent of NTE. In view of all this, it is evident that there is a need to extend the current work on two-dimensional systems (which would be representative of the projection of the real three-dimensional nanostructure of the crystal) so as to investigate other possible networks. This would expand the existing knowledge on, and the applicability of, the RUM concept to other crystalline systems. In particular, this work presents an analytical model to express the thermal expansion characteristics of novel networks made from units which behave as two-dimensional RUMs, particularly, the ones comprising rectangles and the others comprising rhombi, i.e. systems which can be considered as a more general form of the connected squares RUM model.

2. The model

The systems to be modelled are four more general forms of the well-known two-dimensional RUM models made from connected squares, as shown in figure 1*a*. First, we consider systems where the rigid squares [50] are replaced by rigid rectangles of dimensions $a \times b$ (figure 1*b*,*c*), following which we consider systems where the squares are replaced by rigid rhombi [51] of side lengths $a \times a$ having an internal angle ϕ (figure 1*d*,*e*).

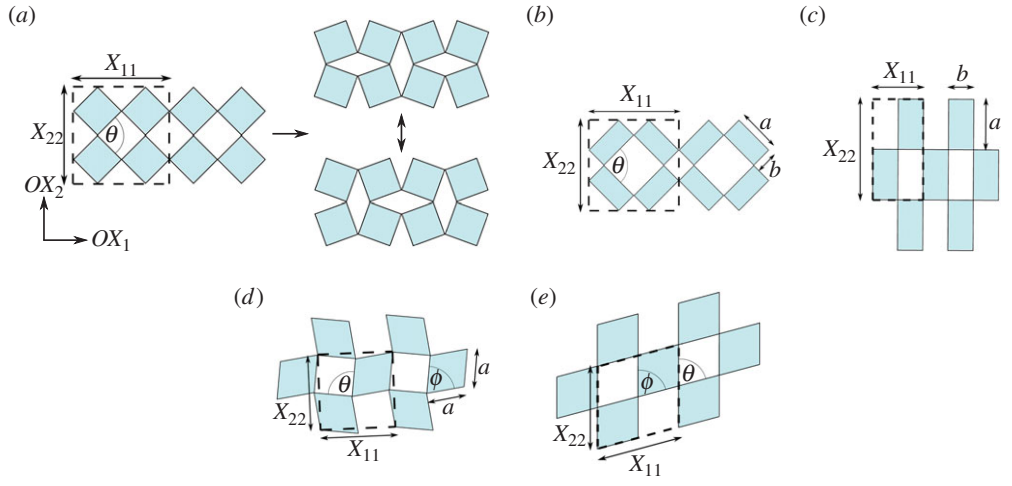

Figure 1. Connected networks composed of (*a*) squares, (*b*) Type I rectangles, (*c*) Type II rectangles, (*d*) Type α rhombi and (*e*) Type β rhombi. The respective RUM for the square-based network is also shown in (*a*); it is assumed that the other geometries follow a similar mode of motion. (Online version in colour.)

In all cases, so as to simplify the analysis and to take a similar approach to the one employed by Dove *et al.* [52], the systems are in their initial 'cold' state (which would correspond to a temperature of 0 K) and the respective rigid units are arranged such that the systems are in their most open conformation where the angle between the rigid units is equal to θ_0. This means that, once heated, the rigid units are expected to start vibrating around this mean conformation. It shall also be assumed that the units behave as harmonic oscillators vis-à-vis rotations, such that at some temperature T, they vibrate about the mean angle, θ_{eq} in a symmetric manner. Given the nature of the systems considered, as well as the potential used, the angles θ_0 and θ_{eq} coincide, meaning that $\theta_0 = \theta_{eq}$. The symmetry of this harmonic potential means that the thermal average of the tilt angle, $\langle \Delta\theta \rangle_T$, may henceforth be assumed to equal zero and the average square of this quantity, $\langle \Delta\theta^2 \rangle_T$, has a non-zero finite value. We also assume that the thermal fluctuations that the system experiences results in very small rotations of the units, so that small angle approximations may be applied to trigonometric functions involving the term $\Delta\theta$.

In the case of the system made up from rectangles of dimensions $a \times b$, as illustrated in figure 1*b*, one may construct two types of networked structures (henceforth referred to as Type I and Type II [53], illustrated in figure 1*b* and *c*, respectively), which differ from each other in terms of their connectives and resultant symmetries. In the case of the network having a Type I connectivity, the whole system can be adequately described through a rectangular unit cell, whose lattice vectors **a** and **b** are represented by $(X_{11}, 0)$ and $(0, X_{22})$, respectively (figure 1*b*). X_{11} and X_{22} are the projections of the unit cell along the Ox_1 and Ox_2 direction and are given by

$$X_{11} = 2\left[a\cos\left(\frac{\theta}{2}\right) + b\sin\left(\frac{\theta}{2}\right)\right] \tag{2.1}$$

and

$$X_{22} = 2\left[a\sin\left(\frac{\theta}{2}\right) + b\cos\left(\frac{\theta}{2}\right)\right]. \tag{2.2}$$

Multiplying the two projections together, one obtains the area of the unit cell, A, at any angle θ:

$$A(\theta) = X_{11}X_{22} = 2(a^2 + b^2)\sin(\theta) + 4ab. \tag{2.3}$$

Expressing θ in terms of an initial angle θ_0 (which is also the equilibrium angle) and a change in the angle $\Delta\theta$, then the area at an angle $\theta_0 \pm \Delta\theta$ is, after simplifying, as follows:

$$A(\theta_0 \pm \Delta\theta) = 2(a^2 + b^2)\sin(\theta_0 \pm \Delta\theta) + 4ab. \tag{2.4}$$

For the system built from rectangles which initially is in its fully open state, i.e. $\theta_0 = \pi/2$, and as for a given $\Delta\theta : \sin(\pi/2 + \Delta\theta) = \sin(\pi/2 - \Delta\theta) = \cos(\Delta\theta)$, then the area function is symmetric, implying that $A(\theta_0 + \Delta\theta) = A(\theta_0 - \Delta\theta)$. Thus, for this particular case when $\theta_0 = \pi/2$, after applying the small angle approximation, one may rewrite the average unit cell area at a temperature T, $\langle A\rangle_T$, as

$$\begin{aligned}\langle A\rangle_T &= 2(a^2 + b^2)\cos(\Delta\theta) + 4ab \\ &\approx 2(a^2 + b^2)\left(1 - \frac{\langle\Delta\theta^2\rangle_T}{2}\right) + 4ab.\end{aligned} \tag{2.5}$$

This applies for a system undergoing angle changes of $\pm\Delta\theta$ as a result of thermal fluctuations corresponding to the temperature T, where $\langle\Delta\theta^2\rangle_T$ is the thermal average of the changes in the term $\Delta\theta^2$ at a temperature T.

The term $\langle\Delta\theta^2\rangle_T$ may be replaced by a term involving temperature through the use of a methodology which is based on the work by Dove *et al.* [52]. In this approach, the average of the squared values of the deviations from the equilibrium position (θ_{eq}) have a non-zero value that is related to the temperature through the principle of equipartition of energy. This principle states that in thermal equilibrium, each independent mode in which energy can be stored is awarded $\frac{1}{2}k_BT$ of energy, where k_B is the Boltzmann constant. Through simple harmonic motion, we know that the energy is distributed into potential and kinetic energy, which continuously interchange. The dynamic energy of a molecule depends on the square of a relative dynamical quantity, which may be a velocity term or displacement. Therefore, as it is being assumed that changes in temperature excite only a single vibrational mode through rotational motion, one may deduce an equation for the potential energy, caused by rotations due to thermal fluctuations of $\Delta\theta$ [52]:

$$\frac{1}{2}I\omega^2\langle\Delta\theta^2\rangle_T = \frac{1}{2}k_BT, \tag{2.6}$$

where ω is the angular frequency of the rotational motion, $\langle\Delta\theta^2\rangle_T$ is the thermal average of $\Delta\theta^2$ and I is the moment of inertia of each rigid unit, a property which depends highly on the distribution of mass around the rotational axis.

Thus, in this particular case, taking the thermal average of the area, and relating it to temperature using equation (2.6), gives

$$\langle A\rangle_T = 2(a^2 + b^2)\left(1 - \frac{k_BT}{2I\omega^2}\right) + 4ab. \tag{2.7}$$

Differentiating $\langle A\rangle_T$ with respect to T, and dividing by $\langle A\rangle_T$, yields the following expression for the area coefficient of thermal expansion, α_A, for the system made from rectangles:

$$\alpha_A = -\frac{k_B(a^2 + b^2)}{I\omega^2(-(a^2 + b^2)(k_B/I\omega^2)T + 2(a^2 + 2ab + b^2))}. \tag{2.8}$$

For this approach to remain valid, the system must behave in a manner where it may be assumed that the units vibrate at a single frequency, ω, which remains unchanged by changes in temperature and therefore volume. This means that a change in temperature results in a change in the amplitude of oscillation, whereas its frequency remains unchanged. This eliminates the need to consider additional modes of vibration, thereby facilitating the treatment of these models.

It may also be shown that for the Type II rectangular systems, where the unit cell is as illustrated in figure 1*c*, the unit cell parameters are given by

$$X_{11} = 2b \sin\left(\frac{\theta}{2} + \frac{\pi}{4}\right) \tag{2.9}$$

and

$$X_{22} = 2a \sin\left(\frac{\theta}{2} + \frac{\pi}{4}\right), \tag{2.10}$$

from which, through a similar approach to the one used above, one may obtain the area coefficient of thermal expansion for the system which is initially in its most open conformation (i.e. where the rectangles are initially at an angle $\theta_0 = \pi/2$, in their 'cold' state)

$$\alpha_A = -\frac{k_B}{I\omega^2(4 - (k_B/I\omega^2)T)}. \tag{2.11}$$

Note that for this connectivity, the area thermal expansion coefficient is independent of the geometrical parameters a and b, and is equal to that derived for the more symmetric case involving the square-based network [52].

Akin to the previous method, one may also derive the properties for the system made from rhombi. Once again, in this case, two systems may be constructed, henceforth referred to as Type α and Type β [53] as illustrated in figure 1*d* and *e*, respectively, depending on the manner by which the rhombi are connected together. In the case of the Type α system, a unit cell contains two rhombi; it has lattice vectors $\mathbf{a} = (X_{11}, 0)$ and $\mathbf{b} = (0, X_{22})$. As depicted in figure 1*d*, X_{11} and X_{22} are the projections of the unit cell along the Ox_1 and Ox_2 direction, and are given by

$$X_{11} = 2a \sin\left(\frac{\phi + \theta}{2}\right) \tag{2.12}$$

and

$$X_{22} = 2a \cos\left(\frac{\phi - \theta}{2}\right). \tag{2.13}$$

By multiplying the two projections together and simplifying, one obtains the unit cell area, which in the case of the Type α rhombi, is given by

$$A(\theta) = 2a^2(\sin(\theta) + \sin(\phi)). \tag{2.14}$$

If this system behaves as above, i.e. at temperature T the rigid units, which are initially at an angle $\theta_0 = \pi/2$ to each other (corresponding to the most open conformation the system can assume), oscillate in a harmonic manner with an angular displacement of $\pm\Delta\theta$, then the area function is symmetric such that $A(\theta_0 + \Delta\theta) = A(\theta_0 - \Delta\theta)$. Thus, using similar approximations to those previously stated, the average unit cell area $\langle A\rangle_T$ at a temperature T may be written as

$$\begin{aligned}\langle A\rangle_T &= 2a^2(\sin(\theta_0 + \Delta\theta) + \sin(\phi)) \\ &= 2a^2(\cos(\Delta\theta) + \sin(\phi)) \\ &\approx 2a^2\left(1 - \frac{\langle\Delta\theta^2\rangle}{2}\right) + 2a^2\sin(\phi) \\ &= 2a^2\left(1 - \frac{k_BT}{2I\omega^2}\right) + 2a^2\sin(\phi).\end{aligned} \tag{2.15}$$

The area coefficient of thermal expansion for this rhombi network may thus be represented by

$$\alpha_A = -\frac{k_B}{I\omega^2(2 - (k_B/I\omega^2)T + 2\sin(\phi))}. \tag{2.16}$$

In the case of the Type β system, whereupon the network is in its most open conformation in the 'cold' state (for which this corresponds to a system where the rhombi are at angle of $\theta_0 = \pi - \phi$ to each other), the area CTE is once again given by equation (2.11), that is independent of the shape and size of the rhombi.

3. Results and discussion

Plots of the variation in the area CTEs with the a/b ratio for the RUM systems made from rectangles of dimension $a \times b$, as well as area CTEs with ϕ for the RUMs systems made from rhombi of internal angle ϕ, are depicted in figure 2. These diagrams clearly show that the systems made from rectangles with the Type I connectivity, and the ones made from rhombi in the Type α connectivity, are capable of exhibiting a high degree of negative area CTE characteristics. This significantly exceeds what may be afforded by the more well-known RUM systems made from squares, or the other systems having a different connectivity (i.e. the Type II rectangles and the Type β rhombi). These plots also suggest the extent of CTE from RUMs may be fine-tuned through changes in the geometric features of the rigid units.

The particular case of the rectangles model where $a = b$, which subsequently converts the rectangles into squares, and the equivalent case where $\phi = \pi/2$ for the rhombic systems, is not the optimal structure for generating NTE, despite the fact that for the past two decades, most researchers have focused their study on this more symmetric structure. However, the expressions and plots also suggest that, for the enhancement in the NTE properties to occur, the relaxation of the constraints where $a = b$ and $\phi = \pi/2$ needs to be done in a careful manner. In fact, the method of connection of the rigid units has a drastic effect on the thermal expansion properties of the systems, with the Type II rectangular or Type β rhombic networks being insensitive to any changes in the shape or size of the respective rectangular/rhombic building blocks.

The enhancement of the NTE properties exhibited by the Type I rectangular or Type α rhombic networks through changes in the geometry brings with it the added benefit of permitting the fine-tuning of the CTE characteristics. This feature is of significant practical importance, as particular application may necessitate the use of materials with some specific thermal expansion profile. Thus, any mechanism which permits the control of the extent of thermal expansion, particularly when the CTE is negative, is highly desirable. In this respect, it is also appropriate to identify the optimal geometric parameters for enhanced NTE. An analysis of equation (2.8) and figure 2*a* suggests that as a/b deviates from unity, particularly when $b \gg a$ or $b \ll a$, the CTE of the Type I rectangles system becomes more negative. This means that as the units elongate and move away from the square symmetry, a greater extent of NTE may be observed. The effect is obviously symmetric in terms of the aspect ratio, meaning that the same CTE values are obtained irrespective of the orientation. One may thus conclude that a network of Type I rectangles having very different a and b values, i.e. in which the rectangles have a 'pencil-like' structure (as illustrated in figure 3), will tend towards maximal NTE. Note that in the limit where the aspect ratio goes to zero (or infinity), this structure would reduce to a molecular wine-rack system, which is well known for its NTE properties [54,55]. Similarly, for the case of the Type α rotating rhombi, the CTE-ϕ plot illustrated in 2*b* depicts that thermal contraction is at a minimum when the rhombi become squares, i.e. at $\phi = \pi/2$. The shape of the plot indicates that the further away the rhombi are from the perfectly symmetric square geometry (i.e. as ϕ tends to 0 or π radians), then the more pronounced the NTE becomes. A Type α rhombic structure having such a low intra-unit angle could also be described as being 'pencil-like'—once more, this system is not too dissimilar from the wine-rack mechanism (figure 4). What is interesting to note is that, irrespective of whether one controls the thermal expansion through changes in the a/b ratio, the intra-unit angle ϕ or the connectivity, those structures having the largest pore size appear to exhibit NTE to the greatest extent. Thus, the emerging pattern is that optimal NTE is best achieved for those rigid structures in which the ratio of *pore area* to *area of solid structure* is maximized. Obviously, in the case of the squares, the maximum area coverage of the pores is just 50% which would correspond to squares in their fully open conformation, where the area of the pores becomes equal to the area of the solid portion. In the case of systems made from Type I rectangles or Type α rhombi, the area occupied by the pores relative to the solid portion may be much higher, tending to 100% as $a/b \to 0, \infty$ in the case of the systems made from rectangles, or $\phi \to 0, \pi$ in the case of the systems made from rhombi. This argument is made stronger by the fact that, in the case of the Type II rectangles or Type β rhombi, the maximum area coverage of

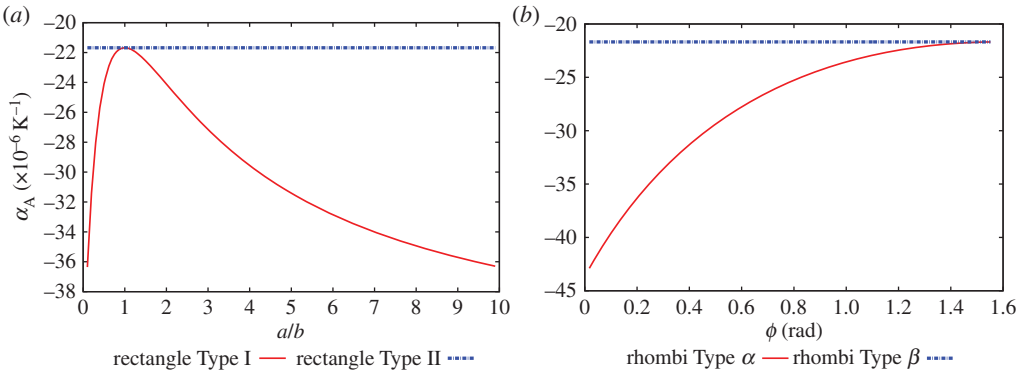

Figure 2. (*a*) Plot of area CTE [$\times 10^{-6}$ K^{-1}] against a/b ratio for rectangular-based networks; (*b*) plot of area CTE [$\times 10^{-6}$ K^{-1}] against ϕ [rad] for networks composed of rhombi. (Online version in colour.)

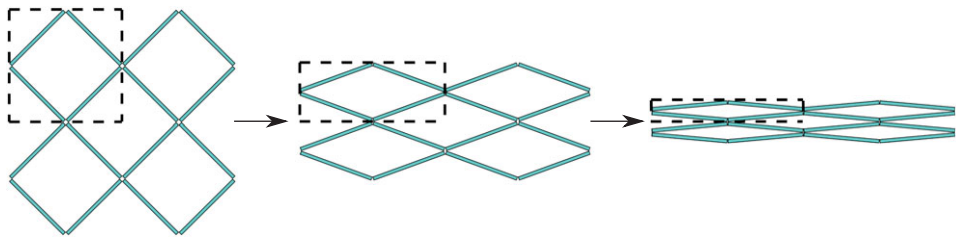

Figure 3. Schematic showing a Type I rectangles network, with very high a/b ratios, on increasing temperature. (Online version in colour.)

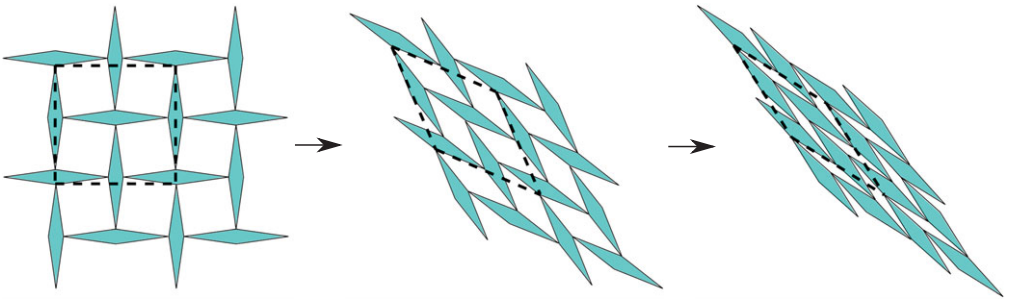

Figure 4. Schematic showing a Type α rhombi network, with a very large intra-unit angle, ϕ, on increasing temperature. (Online version in colour.)

the pores is just 50%—in their most open conformations, the shapes and sizes of the pores would be equivalent to those of the rigid units making up the systems, thus explaining why the CTE properties of the fully open Type II rectangles or Type β rhombi are equivalent to the squares network.

All this is very significant as major efforts are underway in order to design and produce materials with specific thermal expansion properties, as it is well known that a CTE mismatch of the system which is in thermal contact, could result in undesirable, and usually very costly, repercussions. In fact, one of the main uses of NTE materials is to combine them with existing conventional ones so as to adjust the overall thermal expansion coefficient of the resultant material

[56]. In this respect, invar-type materials and other near-zero thermal expansion composite materials (normally composed of negatively and positively expanding materials in the correct ratio), which effectively result in a net expansion coefficient of zero, are of a high practical value [57,58]. This model presents a blueprint which may enable the design of materials with more enhanced NTE characteristics, meaning that smaller quantities of them may be used in the manufacture of real, low or near-zero thermal expansion composites. This would permit for novel formulations where the component that is lowering the thermal expansion is kept to a minimum, thus permitting more flexibility of what the other components in the mixture could be. This could result in the development of superior composites which, apart from having excellent thermal expansion characteristics, could exhibit other remarkable properties such as high strength or extreme thermal/electrical conductivity properties, which would arise from the other components present in the mixture. Such techniques could redefine the materials world, and if economically viable, various engineering problems, such as those related to the fracturing of materials under temperature fluctuations for both large-scale objects used in construction and microelectronic devices used in appliances, could be reduced or even eliminated.

The availability of a mechanical model which builds on geometric features of the materials would be highly advantageous for both researchers and manufacturers alike. For instance, such models could provide chemists with a tool to assist them in the design and synthesis of new NTE materials which, for example, could be built as MOFs [59,60], metal cyanides [61,62] or ceramics [63,64], and optimized so as to achieve some desired thermal expansion property. The applicability or the model presented here to real systems depends to a significant degree on the validity of the assumptions made. For instance, in deriving the model it was assumed that, in accordance with the definition of the CTE, any size or shape change occurs solely as a result of a change in the temperature. Further still, as the model is currently derived, the most important condition is that the system is indeed behaving as one in which its building blocks, or their two-dimensional projection in some particular plane of the material, act as perfectly rigid units. The consequences of this implies that such units may only rotate relative to each other in a rocking-like motion, whereupon the extent of rocking is temperature dependent, increasing as the temperature is increased. This behaviour is clearly too idealistic, as it is well known that increasing the temperature indefinitely would lead to many additional distortions in the crystal structure. Thus, one may argue that the approach used here is slightly over-simplistic, as such idealized behaviour is practically unattainable in real systems. Nevertheless, models such as this one are still essential as they can help identify how, at least in theory, a material should be designed in order to exhibit the required properties. It must be emphasized that even if a material is not behaving in a perfectly ideal manner, the general trends reported here, such as that by smartly modifying the shape of the units experiencing the RUM one could enhance the NTE, would still be applicable. Another consequence of the simplicity of the model is that it is applicable to cases where only one mode is being excited (of constant, average frequency ω).

In reality, this is seldom the case, and usually a number of phonon modes, both acoustic and optical, would be propagating through the structure simultaneously [65]. Each of these would have a particular weighting and therefore, overall effect, on the oscillatory motion of the structure, according to the temperature of the system. For instance, the longitudinal-type stretching modes (propagation along the internuclear axis) would result in a very different motion to that stemming from the aforementioned rocking-modes—thus the extent of NTE would be dependent on which of the modes are excited within the system. Hence, in essence, the other contributions to the thermal expansion from the different vibrational mechanisms acting simultaneously with the rocking-type motion will very likely reduce the negative effects observed and must therefore be accounted for when designing and modelling real materials. It is also important not to use the technique presented here to over-extrapolate information to 'high' temperatures, on account of the incorporation of the 'one-mode' approximation during the derivation of the analytical model.

All this suggests that, a more complex model, based on this preliminary investigation, would need to be formulated so as to better capture the behaviour of real crystalline systems. In such cases, concepts such as RUMs would probably need to be replaced by less restrictive

models, as perfect rigidity is rarely achieved in practice. One such approach is to invoke the concept of the quasi-RUMs (qRUMs) [10,66], in which the units are considered to be semi-rigid, and slight deformations of these respective units are allowed to occur once the rocking-type modes are excited throughout the structure. In addition, it would be more useful to consider three-dimensional models rather than the simpler two-dimensional versions discussed here.

As a final remark, one should not preclude that it could also be theoretically possible to construct metamaterials or nano/micro mechanical devices which would be forced to behave in the manner discussed here. Given the advances that are being made in other areas of metamaterials, this possibility may be closer to achieve now than it was when the original RUM models were proposed more than two decades ago, making the present work much more pertinent. One should equally not preclude that real materials based on the models proposed here could also benefit from other superior properties. In this respect, it should be highlighted that the systems studied here had previously been analysed vis-à-vis their negative Poisson's ratio (auxetic) potential [51,53,67–69] where it was shown that the non-fully open forms of these constructs are able to exhibit the anomalous property of getting wider rather than thinner when uniaxially stretched. Based on the current and earlier work [50,51,53,67,68,70], it is envisaged that one may be able to engineer materials which would be both auxetic and also exhibit NTE characteristics, as has been done via a different paradigm [28,30,71–73] and thus provide a route for the design of new multifunctional materials exhibiting superior thermo-mechanical characteristics. For example, multifunctional (heat and pressure sensitive) materials have the potential to be used in applications involving body armour and protective packaging, whereby the material would react accordingly to changes in the external parameters. For instance, an increase in pressure would cause the material to become thicker, while an increase in temperature would result in a contraction of the system as a whole, in order to safely enclose the contents. In both cases, the reaction of the material would be tailored in such a way as to minimize the potential damage caused to the contents during an accident. Composites that combine the properties of one set of materials with those of another have been widely used in the aerospace industry since the 1950s. The benefit that the industry has derived from them has been the ability to 'tune' materials to survive the range of harsh conditions that aerospace structures meet in service. To illustrate, the functionality of O-rings as used in spacecraft shuttles are very sensitive to changes in temperature and pressure. Adopting a material which may behave in a controlled manner under such fluctuations could lead to an enhancement in safety and performance during flight. However, should one attempt to construct such multifunctional metamaterials, one needs to ensure that the appropriate lengthscale is used. For example, although the equations suggest that the thermal expansion of the rotating rigid rectangles depends on the aspect ratio of the rectangles, macroscopic systems will not exhibit the behaviour analysed here. For this effect to be able to manifest itself, the structural elements must be on the molecular or nanoscale. This is in contrast to the auxetic properties that such systems may afford. These properties can occur at any given lengthscale: ranging from the nanoscale through the microscale, up to the macroscale. In other words, for the thermal fluctuation analysis as described in equations (2.6)–(2.8) to apply, the structural units must be small enough for the vibrational motion to be observable. The frequency ω in equation (2.8) is dependent on the lengthscale and one should obviously not expect a system made from centimetre-sized rhombi or rectangles to vibrate upon heating and demonstrate the NTE effects discussed here.

4. Conclusion

This work has identified more optimal solutions for achieving NTE through RUMs than is presently known. In particular, this work has shown that NTE properties via the RUM mechanism are not just achievable from systems involving squares or equilateral triangles, but from a variety of other geometries. In fact, it was shown that the well-known *rocking squares RUM model*, adopted to explain NTE in a wide variety of materials, is not ideal from a geometrical point of view—a much higher extent of thermal contraction may be achieved from similar networks in which the

squares are replaced by rectangles or rhombi. It was also shown that in such systems, the extent of NTE is dependent, among other things, on the shape of the rigid units used and their respective connectivity. Furthermore, it was found that the extent of NTE can be mapped to the size of the pores in the framework and that for maximum NTE, one would need to use building blocks which have a 'pencil-like' geometry (specifically in this work, by using rectangles with a very high aspect ratio, or rhombi with extreme internal angles). One may envisage that composites and metamaterials designed around the optimized models would have a better chance of exhibiting NTE than those based on previous assessments.

Authors' contributions. J.N.G. conceived the idea, proposed method of analysis and supervised the project. S.S., D.A., M.B. and K.K.D. derived and checked the model. D.A. was involved in the supervision of the project. R.G. was involved in the preliminary work leading to this project. All authors were involved in the discussion and the drafting of the paper.

Competing interests. We declare we have no competing interests.

Funding. This work was supported by the University of Malta.

References

1. White MA. 2012 *Physical properties of materials*, 2nd edn. Boca Raton, FL: CRC Press, pp. 167–182.
2. Scheel K. 1907 Ueber die ausdehnung des quartzglases. *Verh. Dtsch. Phys. Ges.* **9**, 3–23.
3. Mary TA, Evans JSO, Vogt T, Sleight AW. 1996 Negative thermal expansion from 0.3 to 1050 Kelvin in ZrW_2O_8. *Science* **272**, 90–92. (doi:10.1126/science.272.5258.90)
4. Pryde AKA, Dove MT, Heine V. 1998 Simulation studies of ZrW_2O_8 at high pressure. *J. Phys., Condens. Matter* **8417**, 8417–8428. (doi:10.1088/0953-8984/10/38/004)
5. Evans JSO, Mary TA, Sleight AW. 1998 Negative thermal expansion in $Sc_2(WO_4)_3$. *J. Solid State Chem.* **137**, 148–160. (doi:10.1006/jssc.1998.7744)
6. Evans JSO. 1999 Negative thermal expansion materials. *J. Chem. Soc.* **1999**, 3317–3326. (doi:10.1039/A904297K)
7. Mittal R, Chaplot S, Schober H, Mary T. 2001 Origin of negative thermal expansion in cubic ZrW_2O_8 revealed by high pressure inelastic neutron scattering. *Phys. Rev. Lett.* **86**, 4692–4695. (doi:10.1103/PhysRevLett.86.4692)
8. Amos TG, Sleight AW. 2001 Negative thermal expansion in orthorhombic $NbOPO_4$. *J. Solid State Chem* **160**, 230–238. (doi:10.1006/jssc.2001.9227)
9. Allen S, Evans J. 2003 Negative thermal expansion and oxygen disorder in cubic $ZrMo_2O_8$. *Phys. Rev. B* **68**, 134101. (doi:10.1103/PhysRevB.68.134101)
10. Tao J, Sleight A. 2003 The role of rigid unit modes in negative thermal expansion. *J. Solid State Chem.* **173**, 442–448. (doi:10.1016/S0022-4596(03)00140-3)
11. Barrera GD, Bruno JAO, Barron THK, Allan NL. 2005 Negative thermal expansion. *J. Phys. Condens. Matter* **17**, R217–R252. (doi:10.1088/0953-8984/17/4/R03)
12. Zhu J, Andres CM, Xu J, Ramamoorthy A, Tsotsis T, Kotov NA. 2012 Pseudonegative thermal expansion and the state of water in graphene oxide layered assemblies. *ACS Nano* **6**, 8357–8365. (doi:10.1021/nn3031244)
13. Chen K, Song S, Xue D. 2013 Vapor-phase crystallization route to oxidized Cu foils in air as anode materials for lithium-ion batteries. *Cryst. Eng. Comm.* **15**, 144–151. (doi:10.1039/C2CE26544C)
14. Romao CP, Miller KJ, Johnson MB, Zwanziger JW, Marinkovic BA, White MA. 2014 Thermal vibrational, and thermoelastic properties of $Y_2Mo_3O_{12}$ and their relations to negative thermal expansion. *Phys. Rev. B* **90**, 024305. (doi:10.1103/PhysRevB.90.024305)
15. Bruno J, Allan N, Barron T, Turner A. 1998 Thermal expansion of polymers: mechanisms in orthorhombic polyethylene. *Phys. Rev. B* **58**, 8416–8427. (doi:10.1103/PhysRevB.58.8416)
16. Mukherjee M, Bhattacharya M, Sanyal MK, Geue T, Grenzer J, Pietsch U. 2002 Reversible negative thermal expansion of polymer films. *Phys. Rev. E* **66**, 061801. (doi:10.1103/PhysRevE.66.061801)
17. Wang KY, Feng ML, Zhou LJ, Li JR, Qi XH, Huang XY. 2014 A hybrid with uniaxial negative thermal expansion behaviour: the synergistic role of organic and inorganic components. *Chem. Commun.* **50**, 14 960–14 963. (doi:10.1039/C4CC06373B)

18. Woodcock DA, Lightfoot P, Wright PA, Villaescusa LA, Diaz-Cabans MJ, Camblor MA. 1999 Strong negative thermal expansion in the siliceous zeolites ITQ-1, ITQ-3 and SSZ-23. *J. Mater. Chem.* **9**, 349–351. (doi:10.1039/A808059C)
19. Lightfoot P, Woodcock DA, Maple MJ, Villaescusa LA, Wright PA. 2001 The widespread occurrence of negative thermal expansion in zeolites. *J. Mater. Chem.* **11**, 212–216. (doi:10.1039/B002950P)
20. Villaescusa LA, Lightfoot P, Teat SJ, Morris RE. 2001 Variable-temperature microcrystal X-ray diffraction studies of negative thermal expansion in the pure silica zeolite IFR. *J. Am. Chem. Soc.* **123**, 5453–5459. (doi:10.1021/ja015797o)
21. Marinkovic BA, Jardim PM, Rizzo F, Saavedra A, Lau LY, Suard E. 2008 Complex thermal expansion properties of Al-containing HZSM-5 zeolite: a X-ray diffraction, neutron diffraction and thermogravimetry study. *Microporous Mesoporous Mater.* **111**, 110–116. (doi:10.1016/j.micromeso.2007.07.015)
22. Fang H, Dove MT. 2013 Pressure-induced softening as a common feature of framework structures with negative thermal expansion. *Phys. Rev. B* **87**, 214109. (doi:10.1103/PhysRevB.87.214109)
23. Fang H, Dove MT. 2014 A phenomenological expression to describe the temperature dependence of pressure-induced softening in negative thermal expansion materials. *J. Phys. Condens. Matter* **26**, 115402. (doi: 10.1088/0953-8984/26/11/115402)
24. Li H, Eddaoudi M, O'Keeffe M, Yaghi OM. 1999 Design and synthesis of an exceptionally stable and highly porous metal-organic framework. *Nature* **402**, 276–279. (doi:10.1038/46248)
25. Zhou W, Wu H, Yildirim T, Simpson J, Walker A. 2008 Origin of the exceptional negative thermal expansion in metal-organic framework-5 $Zn_4O(1,4\text{-benzenedicarboxylate})_3$. *Phys. Rev. B* **78**, 054114. (doi:10.1103/PhysRevB.78.054114)
26. Rimmer LHN, Dove MT, Winkler B, Wilson DJ, Refson K, Goodwin AL. 2014 Framework flexibility and the negative thermal expansion mechanism of copper(I) oxide Cu_2O. *Phys. Rev. B* **89**, 214115. (doi:10.1103/PhysRevB.89.214115)
27. Schneemann A, Bon V, Schwedler I, Senkovska I, Kaskel S. 2014 Flexible metal-organic frameworks. *Chem. Soc. Rev.* **43**, 6062–6096. (doi:10.1039/C4CS00101J)
28. Lakes R. 2007 Cellular solids with tunable positive or negative thermal expansion of unbounded magnitude. *Appl. Phys. Lett.* **90**, 221905. (doi:10.1063/1.2743951)
29. Steeves CA, dos Santos e Lucato SL, He M, Antinucci E, Hutchinson JW, Evans AG. 2007 Concepts for structurally robust materials that combine low thermal expansion with high stiffness. *J. Mech. Phys. Solids* **55**, 1803–1822. (doi:10.1016/j.jmps.2007.02.009)
30. Romao CP *et al.* 2015 Zero thermal expansion in $ZrMgMo_3O_{12}$: NMR crystallography reveals origins of thermoelastic properties. *Chem. Mater.* **27**, 2633–2646. (doi:10.1021/acs.chemmater.5b00429)
31. Sleight AW. 1998 Negative thermal expansion materials. *Curr. Opin. Solid State Mater. Sci.* **3**, 128–131. (doi:10.1016/S1359-0286(98)80076-4)
32. Kelly A, McCartney LN, Clegg WJ, Stearn RJ. 2005 Controlling thermal expansion to obtain negative expansivity using laminated composites. *Compos. Sci. Technol.* **65**, 47–59. (doi:10.1016/j.compscitech.2004.06.003)
33. Lind C. 2012 Two decades of negative thermal expansion research: where do we stand? *Materials* **5**, 1125–1154. (doi:10.3390/ma5061125)
34. Varghese J, Joseph T, Sebastian MT. 2011 $ZrSiO_4$ ceramics for microwave integrated circuit applications. *Mater. Lett.* **65**, 1092–1094. (doi:10.1016/j.matlet.2011.01.020)
35. Dove MT, Trachenko KO, Tucker MG, Keen DA. 2000 Rigid unit modes in framework structures: theory. *Rev. Mineral. Geochem.* **39**, 1–33. (doi:10.2138/rmg.2000.39.01)
36. Mittal R, Chaplot SL. 2008 Lattice dynamical calculation of negative thermal expansion in ZrV_2O_7 and HfV_2O_7. *Phys. Rev. B* **78**, 174303. (doi:10.1103/PhysRevB.78.174303)
37. Fultz B. 2010 Vibrational thermodynamics of materials. *Prog. Mater. Sci.* **55**, 247–352. (doi:10.1016/j.pmatsci.2009.05.002)
38. Grima JN, Farrugia PS, Gatt R, Zammit V. 2007 A system with adjustable positive or negative thermal expansion. *Proc. R. Soc. A* **463**, 1585–1596. (doi:10.1098/rspa.2007.1841)
39. Tao JZ, Sleight AW. 2003 Free energy minimization calculations of negative thermal expansion in $AlPO_4$-17. *J. Phys. Chem. Solids* **64**, 1473–1479. (doi:10.1016/S0022-3697(03)00102-1)
40. Rimmer LHN, Dove MT, Goodwin AL, Palmer DC. 2014 Acoustic phonons and negative thermal expansion in MOF-5. *Phys. Chem. Chem. Phys.* **16**, 21 144–21 152. (doi:10.1039/C4CP01701C)

41. Barron THK, Berg WT, Morrison JA. 1957 The thermal properties of alkali halide crystals. II. Analysis of experimental results. *Proc. R. Soc. Lond. A* **242**, 478–492. (doi:10.1098/rspa.1957.0190)
42. White GK, Collins JG. 1973 The thermal expansion of alkali halides at low temperatures. II. Sodium, rubidium and caesium halides. *Proc. R. Soc. Lond. A* **333**, 237–259. (doi:10.1098/rspa.1973.0060)
43. Senn MS, Bombardi A, Murray CA, Vecchini C, Scherillo A, Luo X, Cheong SW. 2015 Negative thermal expansion in hybrid improper ferroelectric Ruddlesden-Popper perovskites by symmetry trapping. *Phys. Rev. Lett.* **114**, 035701. (doi:10.1103/PhysRevLett.114.035701)
44. Tautz FS, Heine V, Dove MT, Chen X. 1991 Rigid unit modes in the molecular dynamics simulation of quartz and the incommensurate phase transition. *Phys. Chem. Miner.* **18**, 326–336. (doi:10.1007/BF00200190)
45. Vallade M, Berge B, Dolino G. 1992 Origin of the incommensurate phase of quartz. II. Interpretation of inelastic neutron scattering data. *J. Phys. I* **2**, 1481–1495. (doi:10.1051/jp1:1992223)
46. Swainson IP, Dove MT. 1993 Low-frequency floppy modes in β-Cristobalite. *Phys. Rev. Lett.* **71**, 193–196. (doi:10.1103/PhysRevLett.71.193)
47. Heine V, Welche PRL, Dove MT. 1999 Geometrical origin and theory of negative thermal expansion in framework structures. *J. Am. Ceram. Soc.* **82**, 1793–1802. (doi:10.1111/j.1151-2916.1999.tb02001.x)
48. Grima JN, Chetcuti E, Manicaro E, Attard D, Camilleri M, Gatt R, Evans KE. 2012 On the auxetic properties of generic rotating rigid triangles. *Proc. R. Soc. A* **468**, 810–830. (doi:10.1098/rspa.2011.0273)
49. Pryde AKA, Hammonds KD, Dove MT, Heine V, Gale J, Warren MC. 1996 Origin of the negative thermal expansion in ZrW_2O_8 and ZrV_2O_7. *J. Phys., Condens. Matter* **8**, 10 973–10 982. (doi:10.1088/0953-8984/8/50/023)
50. Grima JN, Evans KE. 2000 Auxetic behavior from rotating squares. *J. Mater. Sci.* **19**, 1563–1565. (doi:10.1023/A:1006781224002)
51. Attard D, Grima JN. 2008 Auxetic behaviour from rotating rhombi. *Phys. Status Solidi B* **245**, 2395–2404. (doi:10.1002/pssb.200880269)
52. Dove MT, Welche PRL, Heine V. 1998 Negative thermal expansion in beta-quartz. *Phys. Chem. Miner.* **26**, 63–77. (doi:10.1007/s002690050161)
53. Grima JN, Manicaro E, Attard D. 2010 Auxetic behaviour from connected different-sized squares and rectangles. *Proc. R. Soc. A* **467**, 439–458. (doi:10.1098/rspa.2010.0171)
54. Grima JN, Gatt R, Alderson A, Evans KE. 2005 On the potential of connected stars as auxetic systems. *Mol. Simul.* **31**, 925–935. (doi:10.1080/08927020500401139)
55. Fortes AD, Suard E, Knight KS. 2011 Negative linear compressibility and massive anisotropic thermal expansion in methanol monohydrate. *Science* **331**, 742–746. (doi:10.1126/science.1198640)
56. Lommens P, De Meyer C, Bruneel E, De Buysser K. 2005 Synthesis and thermal expansion of ZrO_2/ZrW_2O_8 composites. *J. Euro. Ceram. Soc.* **25**, 3605–3610. (doi:10.1016/j.jeurceramsoc.2004.09.015)
57. Lehman J, Lakes RS. 2013 Stiff lattices with zero thermal expansion and enhanced stiffness via rib cross section optimization. *Int. J. Mech. Mater. Des.* **9**, 213–225. (doi:10.1007/s10999-012-9210-x)
58. Lehman J, Lakes RS. 2014 Stiff, strong, zero thermal expansion lattices via material hierarchy. *Compos. Struct.* **107**, 654–663. (doi:10.1016/j.compstruct.2013.08.028)
59. Ryder MR, Civalleri B, Bennett TD, Henke S, Rudic S, Cinque G, Fernandez-Alonso F, Tan JC. 2014 Identifying the role of Terahertz vibrations in metal-organic frameworks: from gate-opening phenomenon to shear-driven structural destabilization. *Phys. Rev. Lett.* **113**, 215502. (doi:10.1103/PhysRevLett.113.215502)
60. Bennett TD, Cheetham AK. 2014 Amorphous metal-organic frameworks. *Acc. Chem. Res.* **47**, 1555–1562. (doi:10.1021/ar5000314)
61. Fang H, Dove MT, Rimmer LHN, Misquitta AJ. 2013 Simulation study of pressure and temperature dependence of the negative thermal expansion in $Zn(CN)_2$. *Phys. Rev. B* **88**, 104306. (doi:10.1103/PhysRevB.88.104306)
62. Cairns AB, Goodwin AL. 2013 Structural disorder in molecular framework materials. *Chem. Soc. Rev.* **42**, 4881–4893. (doi:10.1039/C3CS35524A)

63. Fang H, Dove MT, Phillips AE. 2014 Common origin of negative thermal expansion and other exotic properties in ceramic and hybrid materials. *Phys. Rev. B* **89**, 214103. (doi:10.1103/PhysRevB.89.214103)
64. Grima JN, Attard D, Gatt R. 2011 Unusual thermoelastic properties of methanol monohydrate. *Science* **331**, 687–688. (doi:10.1126/science.1201564)
65. Chaikin PM, Lubensky TC. 2000 *Principles of condensed matter physics*, 1st edn. Cambridge, UK: Cambridge University Press.
66. Hammonds KD, Dove MT, Giddy AP, Heine V, Winkler B. 1996 Rigid-unit modes and structural phase transition in framework silicates. *Am. Mineral.* **81**, 1057–1079.
67. Grima JN, Alderson A, Evans KE. 2005 Auxetic behaviour from rotating rigid units. *Phys. Status Solidi B* **242**, 561–575. (doi:10.1002/pssb.200460376)
68. Attard D, Manicaro E, Grima JN. 2009 On rotating rigid parallelograms and their potential for exhibiting auxetic behaviour. *Phys. Status Solidi B* **246**, 2033–2044. (doi:10.1002/pssb.200982034)
69. Grima JN, Caruana-Gauci R, Attard D, Gatt R. 2012 Three-dimensional cellular structures with negative Poisson's ratio and negative compressibility properties. *Proc. R. Soc. A* **468**, 3121–3138. (doi:10.1098/rspa.2011.0667)
70. Goodwin AL, Kepert CJ. 2005 Negative thermal expansion and low-frequency modes in cyanide-bridged framework materials. *Phys. Rev. B* **71**, 140301. (doi:10.1103/PhysRevB.71.140301)
71. Lakes R. 1996 Cellular solid structures with unbounded thermal expansion. *J. Mater. Sci. Lett.* **15**, 475–477. (doi:10.1007/BF00275406)
72. Grima JN, Farrugia PS, Gatt R, Zammit V. 2007 Connected triangles exhibiting negative Poisson's ratios and negative thermal expansion. *J. Phys. Soc. Jpn.* **76**, 025001. (doi:10.1143/JPSJ.76.025001)
73. Chen J, Xing X, Sun C, Hu P, Yu R, Wang X, Li L. 2008 Zero thermal expansion in $PbTiO_3$-based perovskites. *J. Am. Chem. Soc.* **130**, 1144–1145. (doi:10.1021/ja7100278)